

# Hybrid Polymer Nanoarrays with Bifunctional Conductance of Ions and Electrons and Enhanced Electrochemical Interfaces

Zhangxun Xia,<sup>†,§</sup> Ruili Sun,<sup>†,‡,§</sup> Suli Wang,<sup>\*,†</sup> Luhua Jiang,<sup>†</sup> Hai Sun,<sup>†</sup> and Gongquan Sun<sup>\*,†</sup>

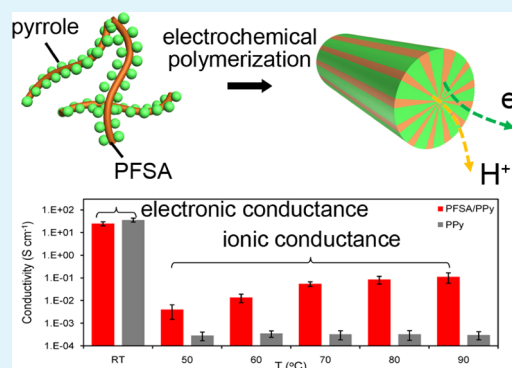
<sup>†</sup>Division of Fuel Cells and Battery, Dalian National Laboratory for Clean Energy, Dalian Institute of Chemical Physics, Chinese Academy of Sciences, Dalian 116023, China

<sup>‡</sup>School of Chemistry and Chemical Engineering, University of Chinese Academy of Sciences, Beijing 100049, China

## Supporting Information

**ABSTRACT:** Ion migration and electron transfer are crucial phenomena in electrochemistry and interfacial sciences, which require effective coupling and integration of separated charge pathways within medium materials. Here, in this work, we fabricated an ordered nanowire material based on hybrid polymers of polypyrrole, with electronic conductance, and perfluorosulfonic acid ionomers, with ionic conductance, via a facile one-step electrochemical route. Because of the nanoconfined effects for the different charge-transfer channels within the nanowire polymer matrix, the electronic and ionic conductivities of the hybrid polymer are surprisingly enhanced, being 26.4 and 0.096 S cm<sup>-1</sup>, respectively. Such an improvement in the formation of charge pathways also leads to an increased electrochemical capacitance through enlargement of the area of ion/electron transport boundaries, which may show great potential in the applications of supercapacitors, fuel cells, rechargeable batteries, and other electrochemical devices.

**KEYWORDS:** conductive polymer, electrochemistry, electrochemical interfaces, ionic conductance, nanomaterials



## INTRODUCTION

Charge transportation, including ion migration and electron transfer, is recognized as a ubiquitous and critical phenomenon in a wide range of natural and technical fields, such as biology, catalysis, electrochemistry, etc.<sup>1–5</sup> For example, the redox reactions in many bioprocesses, such as photosynthesis or nitrogen fixation, are crucially dominated by the construction of proton and electron pathways.<sup>6,7</sup> Also, in electrochemical systems, the formation of reaction boundaries is fundamentally based on the coupling of electronic and ionic conducting phases.<sup>8</sup> In general, the transportation of electrons is basically derived from the movement of free electrons, whereas the environment and pathways for ion transportation are constructed from the ionized molecules or organic groups.<sup>9</sup> Such a fundamental difference leads to separated material fabrication and investigation of ionic and electronic conduction, despite the two processes being synchronized and synergetic in the same electrochemical system in many situations.

In a typical electrochemical system related to most of the energy storage and conversion devices, such as fuel cells, rechargeable batteries, supercapacitors, etc., the formation and structures of the interfaces between the ion- and electron-conductive phases can greatly determine the behaviors and properties of the electrochemical processes.<sup>10,11</sup> The area of the interfaces reflects the spatial capability for electrochemical reactions, and charge transport through the electrode would predominate in the activity of such reactions coupled with ions

and electrons.<sup>12,13</sup> However, electrode construction in most electrochemical devices suffers from the requirement of physically mixing the ion carriers and electronic conductors, resulting in random distribution of the transport structures, which leads to the lack of structural integration and material utilization.<sup>14</sup> Especially for the ions (e.g., protons), the well-defined nanostructures could be crucial for enhancement of transport within a nanoconfined environment.<sup>15–20</sup> Therefore, construction of a composite nanoarchitecture with hybrid pathways for ions and electrons might be a breakthrough in solving these problems and a novel concept for the fabrication of electrodes.

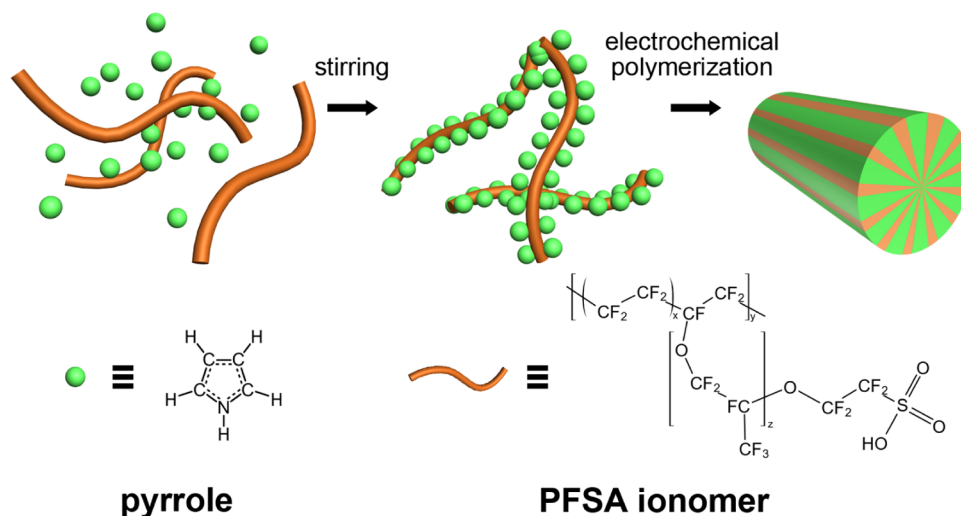
Conductive polymers are a kind of effective electronic conductors with removable  $\pi$ -conjugated electrons,<sup>21</sup> and the organic nature of these materials make them compatible and interactive with other organic molecules or polymers.<sup>22,23</sup> Besides, the optional synthesis methods, for example, electrochemical deposition and chemical oxidation, lead to the formation of hybrid compositions using facile approaches. Herein, we design and fabricate a new nanowire array constructed from a hybrid polymer matrix with polypyrrole (PPy) and perfluorosulfonic acid (PFSA) ionomers via a facile one-step method. The excellent ionic and electronic conductiv-

Received: February 23, 2017

Accepted: May 2, 2017

Published: May 2, 2017

Scheme 1. Schematic of the Synthesis of NfnPPy Nanowires



ities could be detected simultaneously for the homogenous distribution and nanoconfinement of the conductive pathways and the electrochemical properties were greatly enhanced as a result.

## EXPERIMENTAL SECTION

**Synthesis of the Hybrid Polymer.** Hybrid polymer nanowire arrays are prepared via electrochemical polymerization on a platinum (Pt) foil substrate. Briefly, 1.34 g of pyrrole is mixed with 10 g of Nafion ionomer (10 wt % dispersed in water; Sigma Aldrich) and continuously stirred for 12 h at room temperature under a nitrogen atmosphere. The as-prepared mixture is then dissolved in 200 mL of 0.2 M phosphate buffered solution with the addition of 0.1 M *p*-toluenesulfonic acid. A piece of polished Pt foil, a saturated calomel electrode (SCE), and a Pt plate were used as the working electrode, the reference electrode, and the counter electrode, respectively. Electrochemical synthesis was carried out using an electrochemical workstation (SI1287; Solartron) at a constant current of 1 mA cm<sup>-2</sup> for 20 min. Samples of PPy nanowire arrays without Nafion decoration (denoted as PPy) were synthesized in the same manner as the other samples, without the addition of the Nafion ionomer.

**Physical Characterizations.** The as-prepared samples were analyzed via X-ray diffraction (XRD, D/max-2400X; Ricoh), thermogravimetric analysis (Sta 409 PC/PG; Netzsch), and field-emission scanning electron microscopy (JSM-6360LV; JEOL). High-resolution transmission electron microscopy (HRTEM), high-angle annular dark field scanning transmission electron microscopy (HAADF-STEM), and energy dispersive X-ray (EDX) spectroscopy and mapping were carried out with a Tecnai G2 20 microscope (FEI). X-ray photoelectron spectroscopy (XPS) analyses were performed using a Kratos AMICUS spectrometer equipped with a monochromatic Mg X-ray source (Mg K $\alpha$ , 1.2536 keV).

**Electrochemical Measurements.** Electronic conductivity was measured by a traditional two-electrode method (Figure S1), and ionic conductivity was measured by a modified two-electrode method, as illustrated in Figure S2. In brief, the samples were sandwiched by two pieces of Nafion 212 membrane; and then two electrodes coated with Pt/C (40 wt %, 1 mg cm<sup>-2</sup>; Johnson Matthey) were pressed on the Nafion membrane surfaces. The as-prepared test electrode was equipped with flow fields in the end plates. The testing procedures were carried out on an electrochemical workstation (SI1287; Solartron). To achieve potential stability of the electrodes, constant humidified hydrogen flows (0.1 MPa, 20 mL min<sup>-1</sup>) were applied on the both sides through the flow fields. The resistances of the samples were obtained by applying electrochemical impedance spectra and recording the values of the intersection points on the real axis. The conductivity values could be calculated simply with the Ohm's Law. Compared with the traditional

method (Figure S1), this modified measurement could isolate the ionic conductance from the hybrid conductor for both the electron and ion.

Electrochemical characterization was performed in a 0.5 M sulfuric acid solution at room temperature, with a Pt wire and an SCE as the counter electrode and reference electrode, respectively. The scan rate of the cyclic voltammetry (CV) tests is 50 mV s<sup>-1</sup>.

## RESULTS AND DISCUSSION

**Morphological and Structural Details.** Synthesis of the hybrid polymer matrix is illustrated in Scheme 1, and the experimental details are described above. Briefly, after mixing of the conductive polymer monomers (pyrrole) and PFSA ionomers, the pyrrole molecules could be tangled up with the PFSA ionomer chains via interactions between the electro-positive nitrogen of pyrrole and electronegative sulfonate groups of ionomers, and then, the process of electrochemical polymerization is carried out on a piece of conductive substrate (Pt foil). With the help of certain shape-directing reagents, the hybrid polymer matrix could grow on the substrate with the morphology of oriented nanowire arrays.<sup>24</sup> The construction of oriented PPy-based materials has been reported intensively in many other works.<sup>25–27</sup> Briefly, the oppositely charged groups of the shape-directing reagents (e.g., *p*-toluenesulfonic acid) could be attached to the initially formed PPy lines, and then, the hydrophilic sides of the shape-directing reagents would be exposed toward the solution to prohibit horizontal growth of PPy. Similar effects could be also applied to the synthesis of hybrid polymers with Nafion content.

Morphological details of the hybrid polymer nanowire arrays are demonstrated in Figure 1. As shown in the SEM images (Figure 1a,b), a kind of ultrauniform nanowire array is synthesized on the substrate, with an approximate growth density of 3.4 × 10<sup>9</sup> cm<sup>-2</sup>. The typical average length and diameter of the single nanowire is measured as 780 and 83 nm under the electrochemical polymerization conditions mentioned in the Experimental Section. These morphological parameters could be facily controlled via variation of the synthetic conditions, such as temperature, polymerization potential, concentration of the pyrrole monomer, and pH, as described in our previous work.<sup>28</sup> Further analysis of the hybrid polymer on the nanoscale and subnanoscale, as shown in Figure 1c,d, revealed an amorphous structure of the hybrid polymer, without obvious phase separation of the polymers, which also suggests

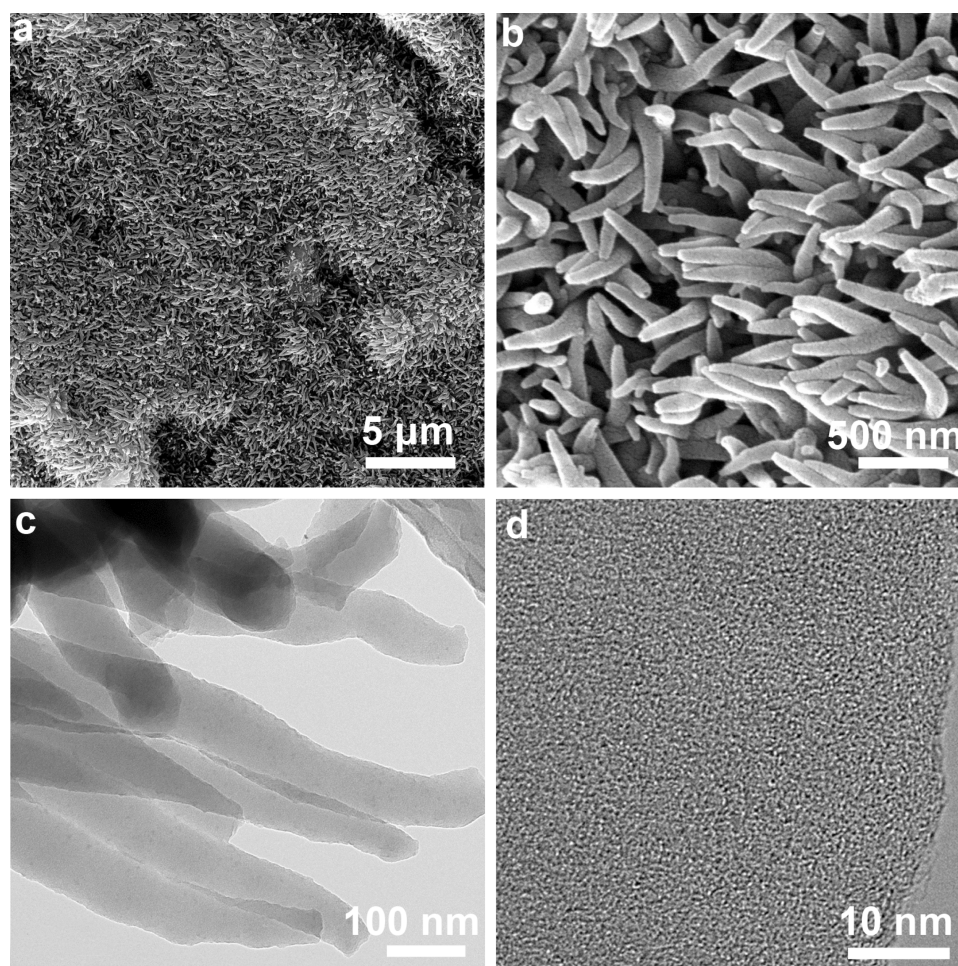


**Figure 1.** Morphological characterization of the hybrid polymers. SEM images (a, b) and HRTEM images (c, d) of the nanowire arrays.

uniform hybridization of the two kinds of polymers during the electrochemical processes.

The compositional information and elementary distribution of the hybrid polymer are investigated by HAADF-STEM and EDX spectral mapping, as shown in Figure 2a,b. The distribution of element N represents the content of PPy, whereas traces of elements F and S suggest the distribution of the PFSA ionomer. The similar and uniform distributions of the PPy and PFSA ionomers reveals that a homogeneous phase of the polymer is constructed from the two compositions during the electrochemical polymerization process. Thermal gravity (TG) analysis (Figure 2c) can also confirm the composition of the PFSA ionomers and PPy in the hybrid polymers. Compared with a single drop in the weight loss curve of the PPy sample (Figure S4), two major drops can be observed at temperatures of 230 and 328 °C, respectively, in the hybrid polymer; the former could be ascribed to the decomposition of PFSA ionomers and the later could be attributed to PPy pyrolysis.<sup>29</sup> The intrinsic structure of the hybrid polymer and pure PPy is further studied by XRD, as shown in Figure 2d. Even though an amorphous structure is observed in the hybrid polymers according to their HRTEM results (Figure 1d), peaks at around 23° in the XRD patterns of the hybrid polymer and PPy sample can be attributed to the semicrystalline structure of the PPy chains, with a typical interplanar distance of 0.39 nm.<sup>24,26</sup> Compared to that of the XRD pattern for the sample of PPy, the peak of the XRD pattern for the hybrid polymer is obviously broadened. This phenom-

enon could be explained by the doping of PFSA ionomer chains into the semicrystalline structure of PPy chains and partial destruction of the long-term ordered structure.<sup>23</sup> Further analyses of the outer space electron structures via XPS tests could also indicate the interactions between PFSA and PPy, as shown in Figure S5. The ratio of N 1s electrons in higher binding energy states ( $-N^+$ ,  $-N=$ ) for PFSA/PPy is increased compared to that for PPy, indicating partial transfer of electrons from polypyrrole molecules to PFSA ionomers. Hence, it is convincing that the structure of the hybrid polymer should be a polymer matrix constructed with PPy chains and PFSA ionomer chains tangled with each other because of the interactions caused by the electrostatic force between the charge-positive nitrogen-containing groups in PPy and the negative sulfonate groups in PFSA ionomers.

**Bifunctional Conductivity.** As a kind of typical electronic conductor for PPy and proton carrier for PFSA, the charge conductance of the hybrid polymer is also derived from the nature of its composing polymers. To detect the electronic and protonic conductivities rationally, a modified measurement is designed. First, the electronic conductivity of the samples could be obtained from measurements using the traditional method, as shown in Figure 3a. The typical magnitude of electronic conductivity for PPy is 10–100 S cm<sup>-1</sup> at room temperature, and the electronic conductivity of the hybrid polymer can also reach such value. This result reveals that hybridization of the composite polymer chains does not significantly reduce the

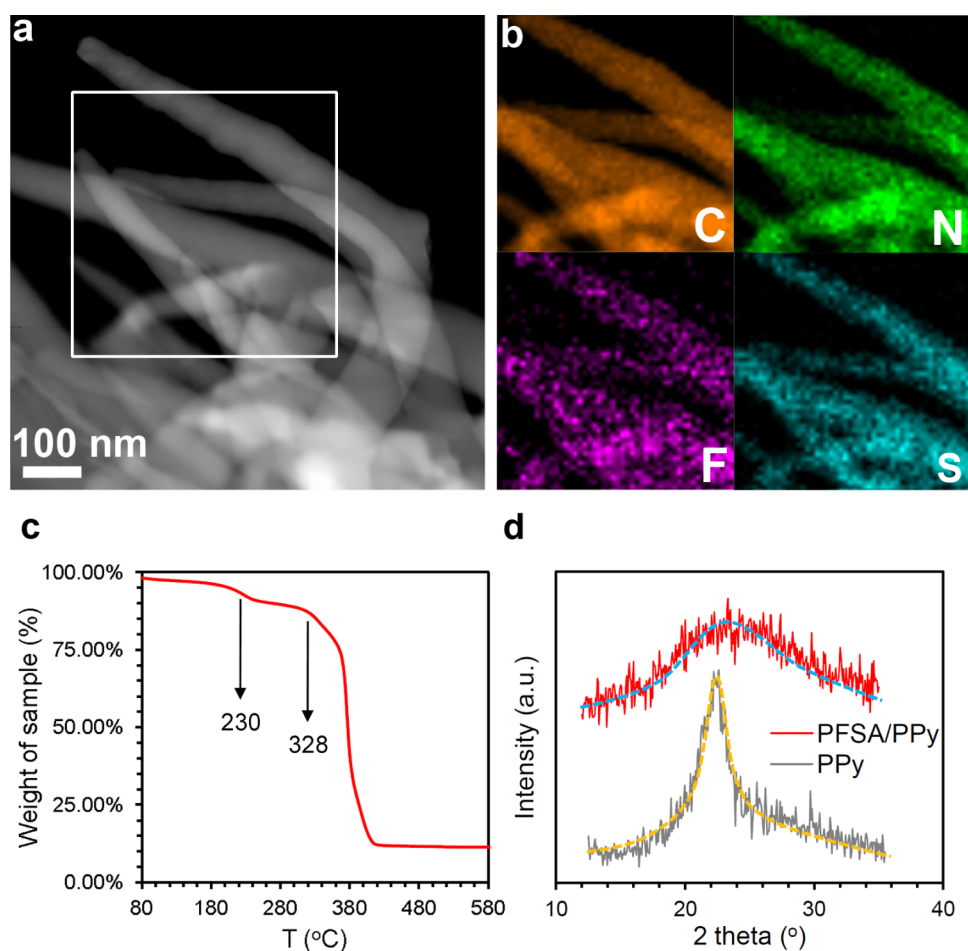


**Figure 2.** (a) STEM and (b) element mapping results of the hybrid polymer nanowires; (c) TG curve of the PFSA/PPy sample and (d) XRD patterns of the PFSA/PPy and PPy samples.

electronic conductance of the conductive polymer originating from the conjugated electron orbits. On the other hand, apart from the nearly ion-insulated PPy sample, the hybrid polymer exhibit remarkable ionic conductance ( $0.0082 \text{ S cm}^{-1}$  at  $50 \text{ }^\circ\text{C}$  and  $0.096 \text{ S cm}^{-1}$  at  $90 \text{ }^\circ\text{C}$ , with a full humidification), which is comparable to that of a typical PFSA membrane (e.g., Nafion membrane). In detail, the ionic conductivity increases with an increase in environmental temperature, which is similar to that for typical PFSA materials. It is noticeable that the PPy sample also possesses a small ionic conductance, which could be derived from the hydrofilm constructed on the hydrophilic surfaces of PPy.<sup>30–32</sup> To explore further details of ion migration through the hybrid polymers, the conductivity data was then transformed into an Arrhenius plot to reveal the relationship between activation energy and ion-transport properties, as shown in Figure 3b. The logarithmic ionic conductivity is approximately linearly correlated to the reciprocal values of temperature, and the activation energy could be calculated from the curve slope according the Arrhenius equation as  $83.27 \text{ kJ mol}^{-1}$ . This value is obviously higher than that for typical PFSA materials (e.g., the  $E_a$  of the Nafion 115 membrane is  $10.8 \text{ kJ mol}^{-1}$ ),<sup>33</sup> which suggests an increased resistance toward proton migration within the transport pathways constructed using the hybrid polymers. The tangled chains of polypyrrole molecules and PFSA ionomers might narrow or obstruct the nanotunnels for proton transport constructed by the hydrophilic groups of the ionomers.<sup>9</sup>

**Electrochemical Property.** To further investigate the electrochemical properties of the hybrid polymers with bifunctional charge transport, electrochemical analysis was performed. The area of the electrochemical interfaces is an important indicator for the performance of the electrodes, especially for electrochemical sensors, fuel cells, rechargeable batteries, and supercapacitors. Hence, CV curves for the hybrid polymer and PPy sample are obtained, as shown in Figure 4a, both of which demonstrate similar patterns, with oxidation and reduction peaks characteristic of PPy-based materials. However, the increased current in the CV curve of the hybrid polymer sample is indicative of a 122% enhancement of the capacitance property compared to that of the PPy sample. Such an increase would indicate an area growth of the ionic/electronic conductor boundaries (or electrochemical surfaces). However, the morphological details for the two samples are similar (Figure S3), which can hardly provide additional surface area for the hybrid polymer in a geometric aspect. Hence, the increased electrochemical surface area should be induced by the internal structures of the hybrid polymer. On the basis of the hybrid matrix structure proposed in the above analysis, the ionic conductive chain of PFSA and the electronic conductive chain of PPy could form a tangled polymer matrix with abundant internal boundaries to extend the electrochemical surfaces from the outer surface, as schematically represented in Figure 4b,c. The hybrid polymer also possesses excellent electrochemical stability, as shown in the similar CV curves before and after 2000 cycles of

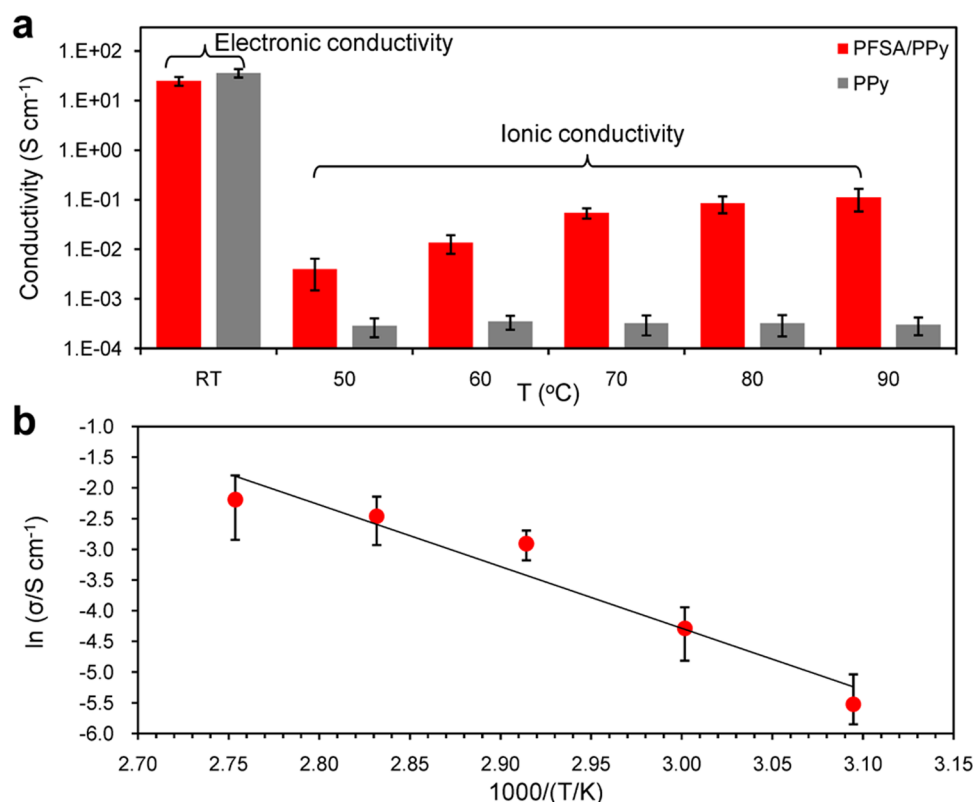


**Figure 3.** (a) Electronic and ionic conductivity of the PFSA/PPy and PPy samples; (b) Arrhenius plot of the ionic conductivity of the hybrid polymer.

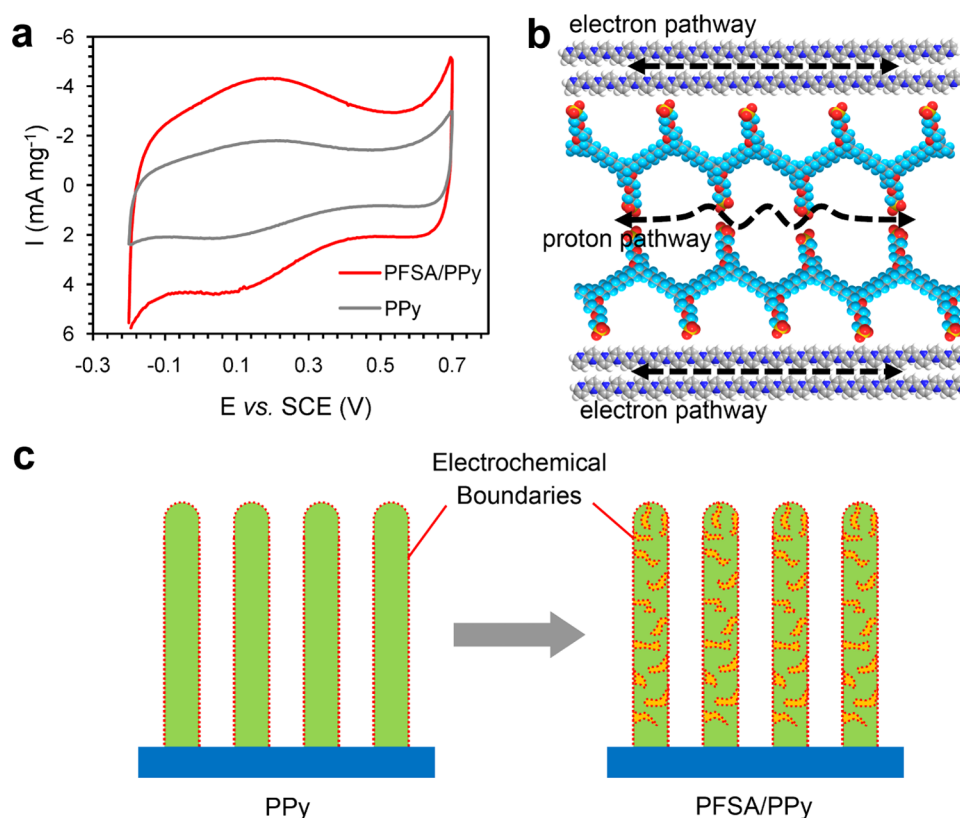


**Figure 4.** (a) CV curves for PFSA/PPy and PPy samples in 0.5 M H<sub>2</sub>SO<sub>4</sub> solution, with a scan rate of 50 mV s<sup>-1</sup>. (b) Schematic of the transport of electrons and protons through the hybrid polymer. (c) Schematic of the increased electrochemical boundaries within the hybrid polymer.

the CV tests in Figure S6. This unique property of the hybrid polymer tailored by the intrinsic structure will be crucial for

electrochemical analysis, and it might be a potential electrode material for many energy-conversion and storage devices.

## CONCLUSIONS

In this work, we demonstrate a kind of hybrid nanofiber polymer with two functions, ionic and electronic conductance, which could be derived from the properties of PFSA ionomers and the conductive polymer (PPy), respectively. These two kinds of linear polymers would be tangled with each other via electrostatic interactions between the sulfonate groups in the PFSA ionomers and nitrogen-containing groups in the PPy chains to form a homogenous polymer matrix through a one-step electrochemical polymerization process. The ionic conductivity of the hybrid polymer is observed to be significantly enhanced by 2 orders of magnitude compared to that of the pure PPy sample, whereas the electronic conductivity is similar for the two samples. As a result of the unique structure of the hybrid polymer matrix, the electrochemical boundaries can be greatly increased by extending the interfaces of the ionic and electronic conducting phases. This property is believed to be critical for the design and construction of electrodes in the future and might shed light on the fundamental and applied aspects of electrochemistry, biomaterials, and energy-conversion techniques.

## ASSOCIATED CONTENT

### Supporting Information

The Supporting Information is available free of charge on the ACS Publications website at DOI: 10.1021/acsami.7b02649.

Schematic of conductivity measurements; SEM and TEM images for the PPy sample; XPS results and CV curves before and after accelerated stress tests (PDF)

## AUTHOR INFORMATION

### Corresponding Authors

\*E-mail: [suliwang@dicp.ac.cn](mailto:suliwang@dicp.ac.cn) (S.W.).

\*E-mail: [gqsun@dicp.ac.cn](mailto:gqsun@dicp.ac.cn) (G.S.).

### ORCID

Zhangxun Xia: 0000-0001-8414-8894

### Author Contributions

<sup>§</sup>Z.X. and R.S. contributed equally to this work.

### Author Contributions

The manuscript was written through contributions of all authors. All authors have given approval to the final version of the manuscript.

### Notes

The authors declare no competing financial interest.

## ACKNOWLEDGMENTS

This work is financially supported by the National Basic Research Program of China (No. 2012CB215500), National Natural Science Foundation of China (No. 21503228), and China Scholarship Council (No. 201604910130). The authors acknowledge Prof. Dang-Sheng Su and Dr. Bingsen Zhang for HRTEM studies and discussions.

## REFERENCES

- (1) Cordes, M.; Giese, B. Electron Transfer in Peptides and Proteins. *Chem. Soc. Rev.* **2009**, *38*, 892–901.
- (2) Ordinario, D. D.; Phan, L.; Walkup, W. G.; Jocson, J. M.; Karshalev, E.; Husken, N.; Gorodetsky, A. A. Bulk Protonic Conductivity in a Cephalopod Structural Protein. *Nat. Chem.* **2014**, *6*, 596–602.
- (3) Salna, B.; Benabbas, A.; Sage, J. T.; van Thor, J.; Champion, P. M. Wide-dynamic-range Kinetic Investigations of Deep Proton Tunnelling in Proteins. *Nat. Chem.* **2016**, *8*, 874–880.

- (4) Weinberg, D. R.; Gagliardi, C. J.; Hull, J. F.; Murphy, C. F.; Kent, C. A.; Westlake, B. C.; Paul, A.; Ess, D. H.; McCafferty, D. G.; Meyer, T. J. Proton-Coupled Electron Transfer. *Chem. Rev.* **2012**, *112*, 4016–4093.

- (5) Kim, Y. B.; Tran-Phu, T.; Kim, M.; Jung, D. W.; Yi, G. R.; Park, J. H. Facilitated Ion Diffusion in Multiscale Porous Particles: Application in Battery Separators. *ACS Appl. Mater. Interfaces* **2015**, *7*, 4511–4517.

- (6) Galloway, J. N.; Dentener, F. J.; Capone, D. G.; Boyer, E. W.; Howarth, R. W.; Seitzinger, S. P.; Asner, G. P.; Cleveland, C. C.; Green, P. A.; Holland, E. A.; Karl, D. M.; Michaels, A. F.; Porter, J. H.; Townsend, A. R.; Vorosmarty, C. J. Nitrogen Cycles: Past, Present, and Future. *Biogeochemistry* **2004**, *70*, 153–226.

- (7) Meyer, T. J.; Huynh, M. H. V.; Thorp, H. H. The Possible Role of Proton-Coupled Electron Transfer (PCET) in Water Oxidation by Photosystem II. *Angew. Chem., Int. Ed.* **2007**, *46*, 5284–5304.

- (8) Maier, J. Nanoionics: Ion Transport and Electrochemical Storage in Confined Systems. *Nat. Mater.* **2005**, *4*, 805–815.

- (9) Mauritz, K. A.; Moore, R. B. State of Understanding of Nafion. *Chem. Rev.* **2004**, *104*, 4535–4585.

- (10) Litster, S.; McLean, G. PEM Fuel Cell Electrodes. *J. Power Sources* **2004**, *130*, 61–76.

- (11) Cho, S.; Shin, K. H.; Jang, J. Enhanced Electrochemical Performance of Highly Porous Supercapacitor Electrodes Based on Solution Processed Polyaniline Thin Films. *ACS Appl. Mater. Interfaces* **2013**, *5*, 9186–9193.

- (12) Qi, L.; Qian, X.; Li, J. Near Neutrality of an Oxygen Molecule Adsorbed on a Pt(111) Surface. *Phys. Rev. Lett.* **2008**, *101*, No. 146101.

- (13) O'Hayre, R.; Prinz, F. B. The Air/Platinum/Nafion Triple-phase boundary: Characteristics, Scaling, and Implications for Fuel Cells. *J. Electrochem. Soc.* **2004**, *151*, A756–A762.

- (14) Borup, R.; Meyers, J.; Pivovar, B.; Kim, Y. S.; Mukundan, R.; Garland, N.; Myers, D.; Wilson, M.; Garzon, F.; Wood, D.; Zelenay, P.; More, K.; Stroh, K.; Zawodzinski, T.; Boncella, J.; McGrath, J. E.; Inaba, M.; Miyatake, K.; Hori, M.; Ota, K.; Ogumi, Z.; Miyata, S.; Nishikata, A.; Siroma, Z.; Uchimoto, Y.; Yasuda, K.; Kimijima, K.-i.; Iwashita, N. Scientific Aspects of Polymer Electrolyte Fuel Cell Durability and Degradation. *Chem. Rev.* **2007**, *107*, 3904–3951.

- (15) Cao, Z.; Peng, Y. X.; Yan, T. Y.; Li, S.; Li, A. L.; Voth, G. A. Mechanism of Fast Proton Transport along One-Dimensional Water Chains Confined in Carbon Nanotubes. *J. Am. Chem. Soc.* **2010**, *132*, 11395–11397.

- (16) Cheruzel, L. E.; Pometun, M. S.; Cecil, M. R.; Mashuta, M. S.; Wittebort, R. J.; Buchanan, R. M. Structures and Solid-state Dynamics of One-dimensional Water Chains Stabilized by Imidazole Channels. *Angew. Chem., Int. Ed.* **2003**, *42*, 5452–5455.

- (17) Dong, B.; Gwee, L.; Salas-de la Cruz, D.; Winey, K. I.; Elabd, Y. A. Super Proton Conductive High-Purity Nafion Nanofibers. *Nano Lett.* **2010**, *10*, 3785–3790.

- (18) Hu, S.; Lozada-Hidalgo, M.; Wang, F. C.; Mishchenko, A.; Schedin, F.; Nair, R. R.; Hill, E. W.; Boukhvalov, D. W.; Katsnelson, M. I.; Dryfe, R. A. W.; Grigorieva, I. V.; Wu, H. A.; Geim, A. K. Proton Transport Through One-atom-thick Crystals. *Nature* **2014**, *516*, 227–230.

- (19) Jeon, H. G.; Jung, J. Y.; Kang, P.; Choi, M. G.; Jeong, K. S. Folding-Generated Molecular Tubes Containing One-Dimensional Water Chains. *J. Am. Chem. Soc.* **2016**, *138*, 92–95.

- (20) Tunuguntla, R. H.; Allen, F. I.; Kim, K.; Belliveau, A.; Noy, A. Ultrafast Proton Transport in Sub-1-nm Diameter Carbon Nanotube Porins. *Nat. Nanotechnol.* **2016**, *11*, 639–644.

- (21) Lyons, M. E. G. Transport and Kinetics in Electroactive Polymers. In *Advances in Chemical Physics: Polymeric Systems*; Prigogine, I., Rice, S. A., Eds.; John Wiley & Sons, Inc.: Hoboken, NJ, 1996; Vol. 94, pp 297–624.

- (22) Pfluger, P.; Krounbi, M.; Street, G. B.; Weiser, G. The Chemical and Physical-Properties of Pyrrole-Based Conducting Polymers - The Oxidation of Neutral Polypyrrole. *J. Chem. Phys.* **1983**, *78*, 3212–3218.

- (23) Milczarek, G.; Ingnas, O. Renewable Cathode Materials from Biopolymer/Conjugated Polymer Interpenetrating Networks. *Science* **2012**, *335*, 1468–1471.

(24) Xia, Z.; Wang, S.; Li, Y.; Jiang, L.; Sun, H.; Zhu, S.; Su, D. S.; Sun, G. Vertically Oriented Polypyrrole Nanowire Arrays on Pd-plated Nafion (R) Membrane and Its Application in Direct Methanol Fuel Cells. *J. Mater. Chem. A* **2013**, *1*, 491–494.

(25) Debiemme-Chouvy, C. Template-free One-step Electrochemical Formation of Polypyrrole Nanowire Array. *Electrochem. Commun.* **2009**, *11*, 298–301.

(26) He, C.; Yang, C. H.; Li, Y. F. Chemical Synthesis of Coral-like Nanowires and Nanowire Networks of Conducting Polypyrrole. *Synth. Met.* **2003**, *139*, 539–545.

(27) Huang, J.; Wang, K.; Wei, Z. Conducting Polymer Nanowire Arrays with Enhanced Electrochemical Performance. *J. Mater. Chem.* **2010**, *20*, 1117–1121.

(28) Xia, Z. X.; Wang, S. L.; Jiang, L. H.; Sun, H.; Sun, G. Q. Controllable Synthesis of Vertically Aligned Polypyrrole Nanowires as Advanced Electrode Support for Fuel Cells. *J. Power Sources* **2014**, *256*, 125–132.

(29) Bissessur, R.; Liu, P. K. Y.; Scully, S. F. Intercalation of Polypyrrole into Graphite Oxide. *Synth. Met.* **2006**, *156*, 1023–1027.

(30) Okuzaki, H.; Kondo, T.; Kunugi, T. Characteristics of Water in Polypyrrole Films. *Polymer* **1999**, *40*, 995–1000.

(31) Garg, S.; Hurren, C.; Kaynak, A. Improvement of Adhesion of Conductive Polypyrrole Coating on Wool and Polyester Fabrics Using Atmospheric Plasma Treatment. *Synth. Met.* **2007**, *157*, 41–47.

(32) Gabriel, S.; Cécius, M.; Fleury-Frenette, K.; Cossement, D.; Hecq, M.; Ruth, N.; Jérôme, R.; Jérôme, C. Synthesis of Adherent Hydrophilic Polypyrrole Coatings onto (Semi)conducting Surfaces. *Chem. Mater.* **2007**, *19*, 2364–2371.

(33) Gu, S.; He, G. H.; Wu, X. M.; Li, C. N.; Liu, H. J.; Lin, C.; Li, X. C. Synthesis and Characteristics of Sulfonated Poly(phthalazinone ether sulfone ketone) (SPPEK) for Direct Methanol Fuel Cell (DMFC). *J. Membr. Sci.* **2006**, *281*, 121–129.